

A Filter Design Approach for Consistent Image Quality

Ahmed H. Eid, Michael J. Phelps and Brian E. Cooper; Lexmark International, Inc.; Lexington, KY, USA

Abstract

In this paper, we propose a system to automatically design image filters, for manufacturers of image capture devices to maintain desired image quality. The proposed system is based on measuring the Spatial Frequency Response (SFR) of the device using the slanted edge technique. This includes an automatic approach to crop the slanted edges and perform the measurements. Based on the measured SFR, an equalizing filter is automatically designed for the device to standardize its SFR to meet a certain goal, for example, to provide unity gain for low and middle frequency ranges while attenuating higher frequencies. In this way, different devices can share an equivalent frequency response and thus offer consistent image quality. A set of device-independent filters may then be cascaded with the equalizing filter of each device. These device-independent filters are designed once, while the numerous individual device-dependent filters are designed automatically. This procedure saves significant effort designing a large collection of individual filters, while improving the consistency of image quality across different image capture devices. To accommodate SFR variation after manufacturing, an end user could apply this approach, if embedded within the device.

Introduction

Image filters are key components of an image processing pipeline to enhance image quality for image capture devices. Image noise removal and edge sharpening/deblurring are the primary use for digital image filters. However, an image pipeline may require the design of many filters (hundreds or even thousands) to provide different quality levels to accommodate various user preferences, workflow requirements, compression levels, and other factors. Designing or even selecting such a large number of unique filters is a long process requiring image quality experts to maintain the desired output image quality.

Although the intended behavior of these filters may involve a degree of subjectivity, consistent behavior is desired across a customer's entire collection of printer and copier models. Maintaining a consistent frequency response for the desired level of image quality is hard to achieve among different devices due to variations in optical components during manufacturing. Degradation of the optical system from aging or environmental factors could mandate redesigning filters by the user or service technician, to maintain the desired quality. Solutions for both cases are possible with a system that can automatically measure and track variations or degradation in the optical system and design appropriate filters accordingly.

In this paper, we propose a system to automatically design image filters during manufacturing, to maintain the desired image quality. This system can be extended to field usage, by embedding its features within the image capture device. Moreover, this system, if adopted by multiple manufacturers, can be extended to a broader range of users in a standardized approach.

The proposed system is based on measuring the Spatial Frequency Response (SFR) of the device using the slanted edge technique [1–4]. This includes an automatic approach to crop the slanted edges and perform the measurement. Based on the measured SFR, an equalizing filter is automatically designed for the device to standardize its SFR to meet a certain goal. For example, the goal SFR may have unity gain for low and middle frequency ranges while attenuating higher frequencies. Applying this procedure to a set of different devices can equalize the SFR of the set. Because they are equalized to a common SFR, the devices should offer similar image quality in terms of their shared frequency response.

A set of device-independent filters may then be cascaded with the equalizing filter of each device. These device-independent filters are designed once. Likewise, only one equalizing filter (for each device resolution) is required for each device and capture mode. Since these equalizing filters unify the device responses, there should be no need to re-design the myriad individual filters required by each unique device and mode. Thus, the output for any given device-independent filter should remain similar across the entire set of image capture devices. This procedure can save considerable effort and allow consistent image quality across multiple devices.

To accommodate variation of the device SFR over the life of the device (or due to component replacements), an end user or service technician could run this procedure as needed. In this case, the device could include the necessary software (for example, embedded within the device) along with a specialized test target to measure the SFR. For scanners, the test target could be integrated with the underside of the scanner lid.

The experimental results section of this paper shows test cases having different frequency responses with the results of applying the proposed system to achieve consistent image quality across devices. A sharpness measure shows that applying the designed filters to various devices with different SFRs can adjust their output images to a similar level of quality.

This paper is organized as follows. The System Overview section describes the system components. The Filter Characteristics section describes how we extract the filter characteristics by measuring the devices' SFRs. The Quality Filter Design section describes the process of designing quality filters using a two-step optimization technique. The final sections are the Experimental Results and Conclusions.

System Overview

In this section we provide an overview of the proposed system (Figure 1). A test target is captured by the scanning device. We use the slanted edge test chart [3], as shown in Figure 2(a). The slanted edge technique is an ISO standard approach to measure the spatial frequency response (SFR) (both horizontal and vertical) of digital imaging devices [1–6].

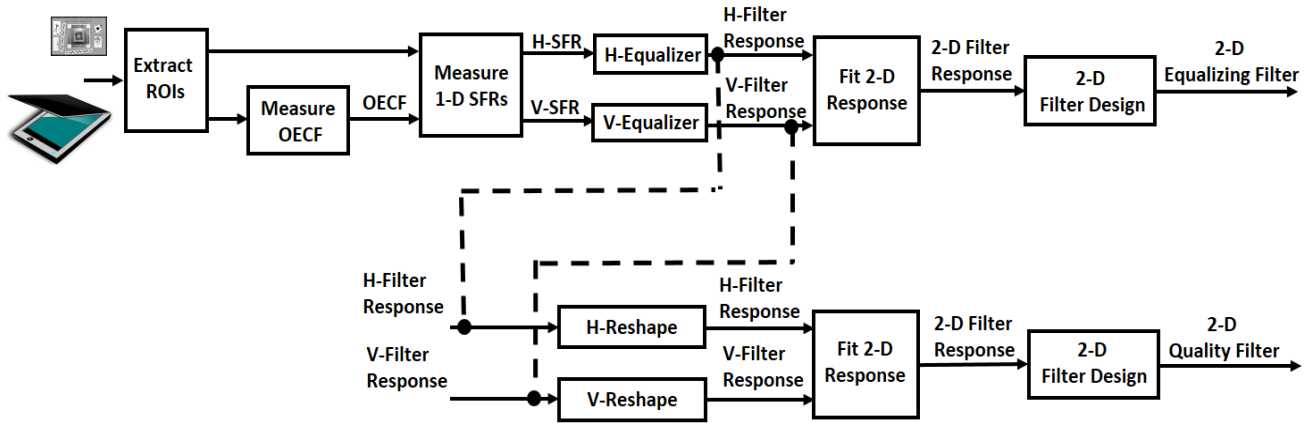


Figure 1. Proposed system block diagram.

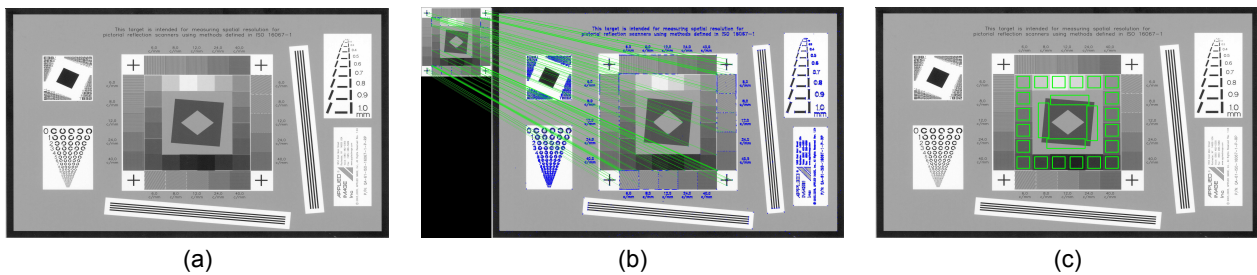


Figure 2. Slanted edge measurements: (a) ISO 16067-1 slanted edge test chart [3], (b) Green lines indicate matches between reference target (upper-left corner) and scanned target, and (c) Green rectangles show identified regions in scanned target.

We measure the Opto-Electronic Conversion Function (OECF) [7] for tone adjustment of different scanners. The slanted edge target includes 24 patches of gray shades to measure the OECF. We automatically detect both the 24 patches and the horizontal and vertical slanted edges using the local image descriptor BRISK [8, 9]. First, we detect and store the local image descriptors of keypoints of the slanted edge reference target. Then we match the reference keypoints to the detected keypoints of the newly scanned target, as shown in Figure 2(b). The match determines the geometric transformation that maps the locations of known regions of the reference target (containing the slanted edges and gray patches) into the corresponding regions in the new scanned target. (Although the geometric transformation can accommodate a perspective distortion, an affine transform is sufficient for scanners.) Using the detected slanted edges and gray patches in the scanned target (as shown in Figure 2(c)), we can then measure both OECF and SFRs of the scanner.

As shown in Figure 1, to measure the blur characteristics of the scanning device, we measure the horizontal and vertical SFRs of the scanner. Starting from the measured SFR of the scanning device, our goal is to design an equalizing filter so that the combined SFR of the filter and the scanner resembles a particular goal SFR, G . For example, we chose a goal SFR with unity gain from zero frequency up to a desired frequency, with gradual attenuation thereafter to limit high-frequency noise. To get the unity section, the equalizing filter response should be the inverse of the original SFR of the scanner within that section. We choose the frequency

band of the unity section to be $[0, f_s/4]$, where f_s is the spatial sampling frequency. The attenuation section is chosen to be linear, such that the frequency response reaches zero at frequency $f_s/2$.

The desired 2D frequency response of the filter is computed using linear interpolation of the 1D horizontal and vertical responses derived from the corresponding SFRs of the scanner. The filter design technique has two steps. First, a linear system of equations is constructed using the unknown filter coefficients and the desired filter 2D response. A zero-phase filter and symmetrical point spread function are assumed for simplicity. The linear least squares method is used to solve the linear system of equations.

The second step of the filter design uses a nonlinear optimization technique to refine the results of the first step. An energy functional with two terms is proposed. The first term is a weighted sum of squared errors with higher weights assigned to mid-range frequencies, around $f_s/4$, where the highest gain occurs. Also, the filter's stop-band is assigned a higher weight to assure the desired attenuation at high frequencies. The second term of the energy functional is a regularized exponential term, defined as a function of the sum of filter coefficients. This ensures zero-frequency (DC) unity gain, to preserve the average image intensity. We use the Nelder-Mead, downhill simplex optimization technique to iteratively find optimal filter coefficients [11].

Other options are available for the goal SFR. For example, rather than using unity gain, the goal SFR could provide a certain

level of image sharpening. The equalizing filters assure that all scanners will share similar sharpening behavior. Of course, other behaviors are possible with other choices of the goal SFR.

To attain different image quality levels, a set of pre-specified frequency reshaping curves can be cascaded with the equalizing frequency curves. In this case, instead of designing an equalizing filter, we design a set of quality filters (to achieve desired quality) based on the product of the equalizing frequency response and the reshaping frequency specifications, as shown in the bottom portion of Figure 1. Thus, to design new filters for new scanning devices, our approach requires only the measurement of the scanner's SFR, eliminating the significant effort of designing numerous individual filters. From this, we can automatically compute the corresponding scanner-dependent equalizing filter or reshaping filters.

The pre-specified reshaping curves are designed once, using a reference scanner. Each reshaping curve satisfies a particular design goal, adjusting the frequency response to offer the desired image quality. The reshaping curves are derived by dividing each quality filter's frequency response by the equalizing filter's response measured from the reference scanner. These reshaping curves are then used with future scanners to achieve similar quality levels as described above.

Filter Characteristics

In this section we describe how filter characteristics are extracted using measurements from scans of the slanted edge test chart [3]. To find the equalizing filter response we invert the measured SFR, both horizontal (SFR_u) and vertical (SFR_v), of the scanner in the frequency range 0 to $f_s/4$ and linearly attenuate the higher frequencies in the range $f_s/4$ to $f_s/2$ such that the frequency response reaches zero at $f_s/2$. The equalizing frequency response T_u in the horizontal direction can be described as:

$$T_u(u) = \begin{cases} \frac{1}{SFR_u(u)}, & 0 \leq u \leq u_s/4 \\ m_u(u - u_s/4) + \frac{1}{SFR_u(u_s/4)}, & u_s/4 \leq u \leq u_s/2 \end{cases} \quad (1)$$

where u_s is the horizontal spatial sampling frequency and m_u is defined as:

$$m_u = \frac{4}{u_s} \left(k_u - \frac{1}{SFR_u(u_s/4)} \right)$$

where k_u is an arbitrary constant that defines the value of T_u at $u = u_s/2$. In our analysis we use $k_u = 0$ which reduces m_u to:

$$m_u = -\frac{4}{u_s SFR_u(u_s/4)}$$

and $T_u(u)$ to:

$$T_u(u) = \begin{cases} \frac{1}{SFR_u(u)}, & 0 \leq u \leq u_s/4 \\ -\frac{4u}{u_s SFR_u(u_s/4)} + \frac{2}{SFR_u(u_s/4)}, & u_s/4 \leq u \leq u_s/2 \end{cases} \quad (2)$$

A similar derivation of the equalizing vertical response T_v can be written as:

$$T_v(v) = \begin{cases} \frac{1}{SFR_v(v)}, & 0 \leq v \leq v_s/4 \\ -\frac{4v}{v_s SFR_v(v_s/4)} + \frac{2}{SFR_v(v_s/4)}, & v_s/4 \leq v \leq v_s/2. \end{cases} \quad (3)$$

where v_s is the vertical spatial sampling frequency. Thus, T_u and T_v satisfy the required goal that $T_u SFR_u = G_u$ and $T_v SFR_v = G_v$,

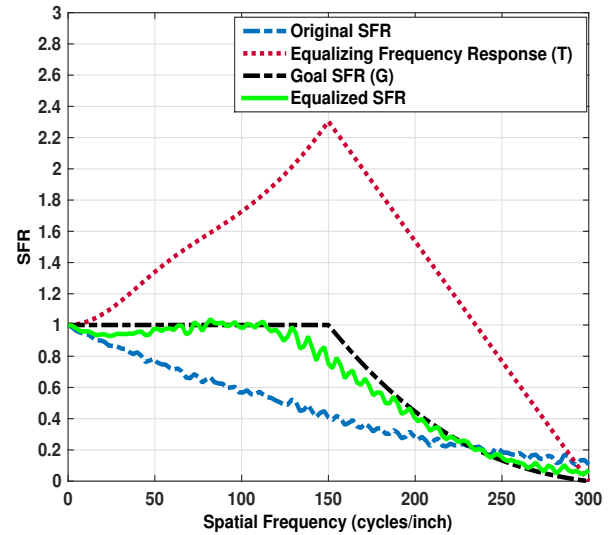


Figure 3. Examples of a measured SFR, corresponding equalizing frequency response, goal SFR and the equalized SFR.

where G_u and G_v are the goal SFRs in each direction. Figure 3 shows examples of a measured (original) SFR, its corresponding equalizing response T , its equalized frequency response, and the goal SFR G .

Based on the desired quality frequency reshaping curves, R_u and R_v can be cascaded with the equalizing responses (T_u and T_v , respectively) to find the final characteristics Q_u and Q_v of quality filters as

$$Q_u(u) = T_u(u)R_u(u) \quad (4)$$

and

$$Q_v(v) = T_v(v)R_v(v) \quad (5)$$

Thus, $Q_u SFR_u = (T_u SFR_u)R_u = G_u R_u$ and $Q_v SFR_v = (T_v SFR_v)R_v = G_v R_v$. This allows the reshaping curves to be independent of the given scanner.

A zero-phase 2D equalizing filter can be derived from the horizontal and vertical frequency samples. First, we find the magnitude of the 2D frequency response, $Q(u, v)$, of the filter by the linear interpolation of the horizontal and vertical samples. Using Fourier transform equations, unknown filter coefficients can be computed optimally by minimizing the error between the target and the modeled frequency responses of the filter as described in the next section.

Quality Filter Design

For an $M \times N$ filter, the frequency response $H(u, v)$ can be expressed in terms of the filter's coefficients (impulse response) $h(m, n)$ using a Fourier transform as: [11]

$$H(u, v) = h(0, 0) + \sum_{(m,n) \in R_1} h(m, n) e^{-j2\pi m \frac{u}{f_m}} e^{-j2\pi n \frac{v}{f_m}} + \sum_{(m,n) \in R_2} h(m, n) e^{-j2\pi m \frac{u}{f_m}} e^{-j2\pi n \frac{v}{f_m}} \quad (6)$$

where R_1 and R_2 are regions of support of $h(m, n)$ and f_m is $\max(u_s, v_s)$. For zero phase filters, R_2 is R_1 flipped with respect to the origin where $h(m, n) = h(-m, -n)$ [10]. Therefore, the frequency response of a twofold symmetry filter can be expressed as:

$$H(u, v) = h(0, 0) + \sum_{(m, n) \in R_1} h(m, n) \cos(2\pi m \frac{u}{f_m} + 2\pi n \frac{v}{f_m}) \quad (7)$$

For circularly symmetric filters, a fourfold constraint on $h(m, n)$ can be imposed such that:

$$h(m, n) = h(m, -n) = h(-m, n) = h(-m, -n) \quad (8)$$

which is equivalent to:

$$H(u, v) = H(u, -v) = H(-u, v) = H(-u, -v)$$

Due to this symmetry, the number of independent filter coefficients is $(M+1)(N+1)/4$ if M and N are odd numbers.

To solve for unknown filter coefficients $h(m, n)$ in Eq. 7 with the constraints in Eq. 8, given target frequency response $Q(u, v)$, we use the singular value decomposition (SVD) technique to find

$$\arg \min_{h_I(m, n)} \frac{1}{2} \sum_{u, v} (Q(u, v) - H(u, v))^2. \quad (9)$$

We use the values of $h_I(m, n)$ as an initial solution to the the second optimization step using the downhill simplex method. We use different weights for errors at different frequency bands. A second term is added to ensure unity gain at zero frequency (DC gain). The final filter coefficients are computed by solving

$$\arg \min_{h_F(m, n)} (\sum_{u, v} \alpha(u, v) (Q(u, v) - H(u, v))^2 + \beta E_0). \quad (10)$$

where

$$\alpha(u, v) = \begin{cases} \alpha_0, & (\frac{u}{u_0})^2 + (\frac{v}{v_0})^2 < 1 \\ \alpha_1, & (\frac{u}{u_0})^2 + (\frac{v}{v_0})^2 \geq 1, (\frac{u}{u_1})^2 + (\frac{v}{v_1})^2 < 1 \\ \alpha_2, & (\frac{u}{u_1})^2 + (\frac{v}{v_1})^2 \geq 1, (\frac{u}{u_2})^2 + (\frac{v}{v_2})^2 < 1 \\ \alpha_3, & (\frac{u}{u_2})^2 + (\frac{v}{v_2})^2 \geq 1 \end{cases} \quad (11)$$

and

$$E_0 = e^{(Q(0,0) - H(0,0))^2} - 1 \quad (12)$$

We use $\alpha_2 = \alpha_0$, $\alpha_3 = \alpha_1 = 5\alpha_0$, and $\beta = 40\alpha_0$. The values of frequency thresholds are selected as:

$$u_0 = 0.05u_s, u_1 = 0.3u_s, u_2 = 0.4u_s$$

and

$$v_0 = 0.05v_s, v_1 = 0.3v_s, v_2 = 0.4v_s$$

for the horizontal and vertical responses, respectively. Optimization stops when reaching either a predefined error limit or the maximum number of iterations.

Experimental Results

In this section, we provide an experiment to show how our method provides consistent output quality for different scanners. We use scans from two different scanners, A and B. We apply a Gaussian filter with two different standard deviations ($\sigma = 0.5$ and $\sigma = 0.6$) to scanner A to simulate scanners with higher blurring characteristics. The goal is to show that the proposed system achieves a good level of consistency of the output frequency responses of the test scanners (and consequently consistent output quality), even when the scanners originally had different characteristics. We show the new SFRs and measure the sharpness of the enhanced scans of the test scanners using the no-reference blur metric from Narvekar and Karam [12].

Measured using the slanted edge technique, the horizontal and vertical SFRs of the test scanners are shown in Figures 4(a) and (b) respectively. These measured SFRs show the difference in test scanner responses, both horizontally and vertically. To equalize these responses we apply equalizing filters with the desired frequency characteristics for both horizontal and vertical directions, as shown in Figure 4(c) and (d), respectively. Thus, the combination of SFR (from Figure 4(a) and (b)) and equalizing filter (from Figure 4(c) and (d)) equals the goal SFR.

Using an equalizing filter (for each scan resolution and mode), we achieve the goal of equalizing scanner responses. However, our ultimate goal is to achieve consistent output quality among different scanners while eliminating the need for the time-consuming process of manually designing image filters for each combination of scanner and reshaping function. To achieve that, we design reshaping curves, for example, as shown in Figure 5. One such reshaping filter (solid green line) is simply a unity filter, which provides an output quality filter that is identical to the equalizing filter. In addition, other reshaping curves can be used to provide sharper or smoother output than the equalizing quality level. Cascading these curves with the equalizing characteristics of Figure 4 leads to the desired characteristics of the final quality filters.

Using the proposed approach, we design the quality filters shown in Figure 6. The top row of Figure 6 shows the quality filters obtained by cascading the individual equalizing characteristics of each scanner with the unity reshaping curve (see Figure 5), so that the filtered frequency response of each scanner equals the goal SFR. Results are shown for scanner A, scanner B, scanner A with $\sigma = 0.5$, and scanner A with $\sigma = 0.6$ in columns (a), (b), (c), and (d) of Figure 6 respectively. Differences in these filters reflect the differences in the original frequency responses of these scanners. The middle and bottom rows of Figure 6 show the quality filter responses of the four tested scanners, after cascading the gain and attenuation curves (see Figure 5), respectively, with the equalizing characteristics. These filter responses also reflect the necessary adjustment for each scanner to achieve consistent quality with the other scanners.

To demonstrate the consistency of frequency responses after applying the quality filters of Figure 6, we measure the SFRs of each scanner, as shown in Figure 7. Generally, the equalized SFRs for the different scanners show very similar responses, as intended. The largest deviation occurs for scanner A with Gaussian blur of $\sigma = 0.6$. (For example, see Figure 7(c) and (d).) Its SFR includes the greatest amount of blur among the evaluated scanners, leading to quality filters with higher gains. This may

cause clipping of the intensity values at the slanted edges, which could affect the results of the slanted edge technique.

The no-reference blur metric (CPBDM) from Narvekar and Karam [12] offers an image quality attribute for us to quantify the sharpness levels for the above filters. Table 1 shows a summary of the CPBDM sharpness measure for each of the four scanners. The corresponding images are shown in Figure 8. In the table, the sharpness values for the original non-equalized values differ according to the sharpness characteristics of each scanner. For example, scanner A with Gaussian blur $\sigma = 0.6$ has the lowest sharpness value. After applying the designed quality filters, the frequency response will be consistent across all scanners, as validated by the consistency in the quantitative sharpness values. Similar sharpness values occur across all four scanners, for each the equalized, equalized with gain, and equalized with attenuation results.

The above results demonstrate that we can achieve consistent image quality for different scanners using the proposed system. However, we mainly focused on image sharpness as an image quality attribute. Although we attenuate very high frequencies to reduce noise, we still amplify noise levels at other frequencies since we apply the designed filters unconditionally to all image contents. Using segmentation techniques to segment edges from images, we can apply the designed filters to sharpen edges and de-noise other contents using smoothing filters. In this case, we can use the proposed system to design all such filters (whether for sharpening or smoothing) to achieve consistent quality for different scanners and different image contents.

Conclusions

In this paper, we propose a system to automatically design image filters to provide consistent image quality among different scanning devices. The proposed system requires measurements of a slanted edge test chart and the design of reshaping frequency curves to provide certain quality levels. Based on these measurements, we design linear equalizing filters to invert the inherent blurring of the scanning process to reach an equalizing response for each scanning device. The equalizing filter assures that each scanner matches the same intended frequency response goal. We then cascade the reshaping curves with these equalizing characteristics. Experimental results show consistent image quality among the evaluated scanners when measuring the image sharpness using a known sharpness measure.

References

- [1] S. Reichenbach, S. Park, and R. Narayanswamy, "Characterizing digital image acquisition devices," *Optical Engineering*, 30(2), 170-177 (1991).
- [2] ISO 12233-1:2014, *Photography — Electronic still-picture imaging — Resolution and spatial frequency responses*, International Organization for Standardization (ISO), (2014).
- [3] ISO 16067-1:2003, *Photography — Spatial resolution measurements of electronic scanners for photographic images — Part 1: Scanners for reflective media*, International Organization for Standardization (ISO), (2003).
- [4] P. D. Burns, "Slanted-edge MTF for digital camera and scanner analysis," *Proc. IS&T 2000 PICS Conference*, 135-138 (2000).
- [5] D. Williams, "Benchmarking of the ISO 12233 slanted-edge spatial frequency response plug-in," *Proc. IS&T 1998 PICS Conference*, 133-136 (1998).
- [6] E. K. Zeise, "Characteristic measurements for the qualification of reflection scanners in the evaluation of image quality attributes." *Proceedings of SPIE/IS&T Electronic Imaging*, Vol. 7242, 724202 (2009).
- [7] ISO 14524:2009, *Photography — Electronic still-picture cameras — Methods for measuring opto-electronic conversion functions (OECFs)*, International Organization for Standardization (ISO), (2009).
- [8] S. Leutenegger, M. Chli, and R. Siegwart, "BRISK: Binary robust invariant scalable keypoints," *2011 IEEE International Conference on Computer Vision (ICCV)*, 2548-2555 (2011).
- [9] opencv: <http://opencv.org/>
- [10] J. S. Lim, *Two-Dimensional signal and image processing*, Prentice-Hall, Upper Saddle River, NJ (1990).
- [11] A. Eid, "A linear filter design technique for equalizing document scanners," *Proceedings of SPIE/IS&T Electronic Imaging*, Vol. 8295, 82950X (2012).
- [12] N. D. Narvekar and L. J. Karam, "A No-Reference Image Blur Metric Based on the Cumulative Probability of Blur Detection (CPBD)," *IEEE Transactions on Image Processing*, 20(9), 2678-2682 (2011).

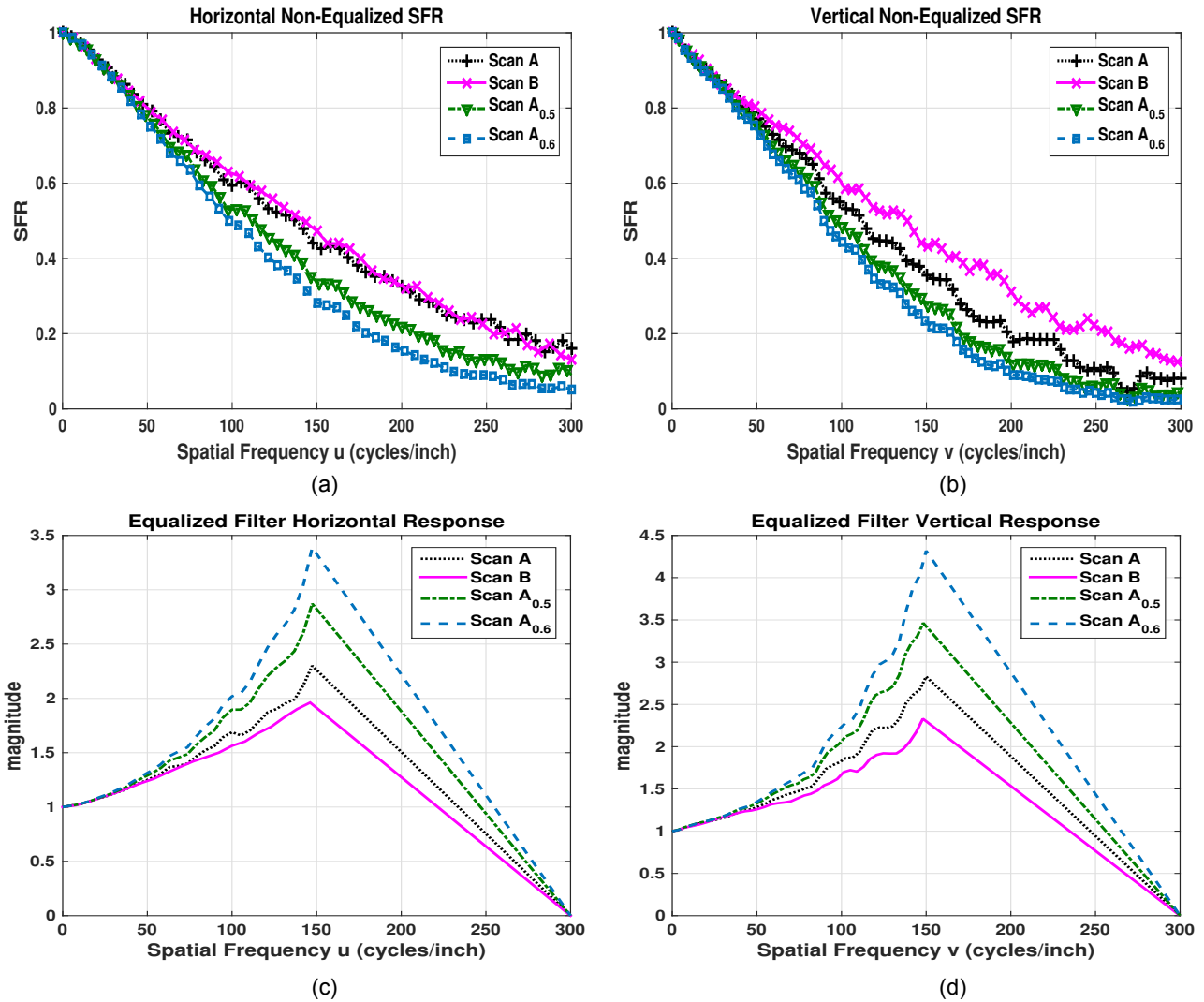


Figure 4. Original SFRs of different scanners in the (a) horizontal and (b) vertical directions, with the corresponding frequency responses of equalizing filters for each scanner in the (c) horizontal and (d) vertical directions.

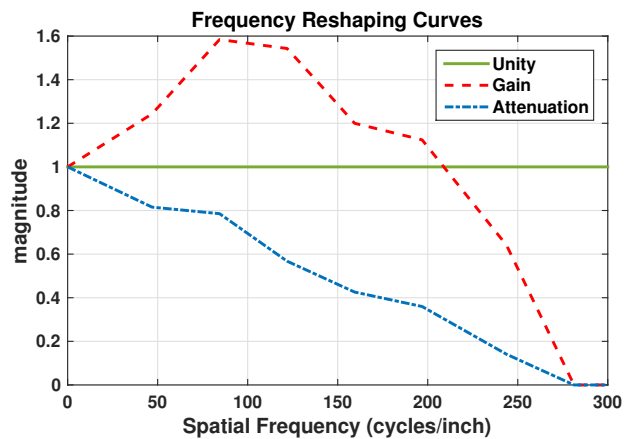


Figure 5. Examples of different reshaping curves to be cascaded with the equalizing characteristics of different scanners to achieve desired quality levels. These curves are device-independent.

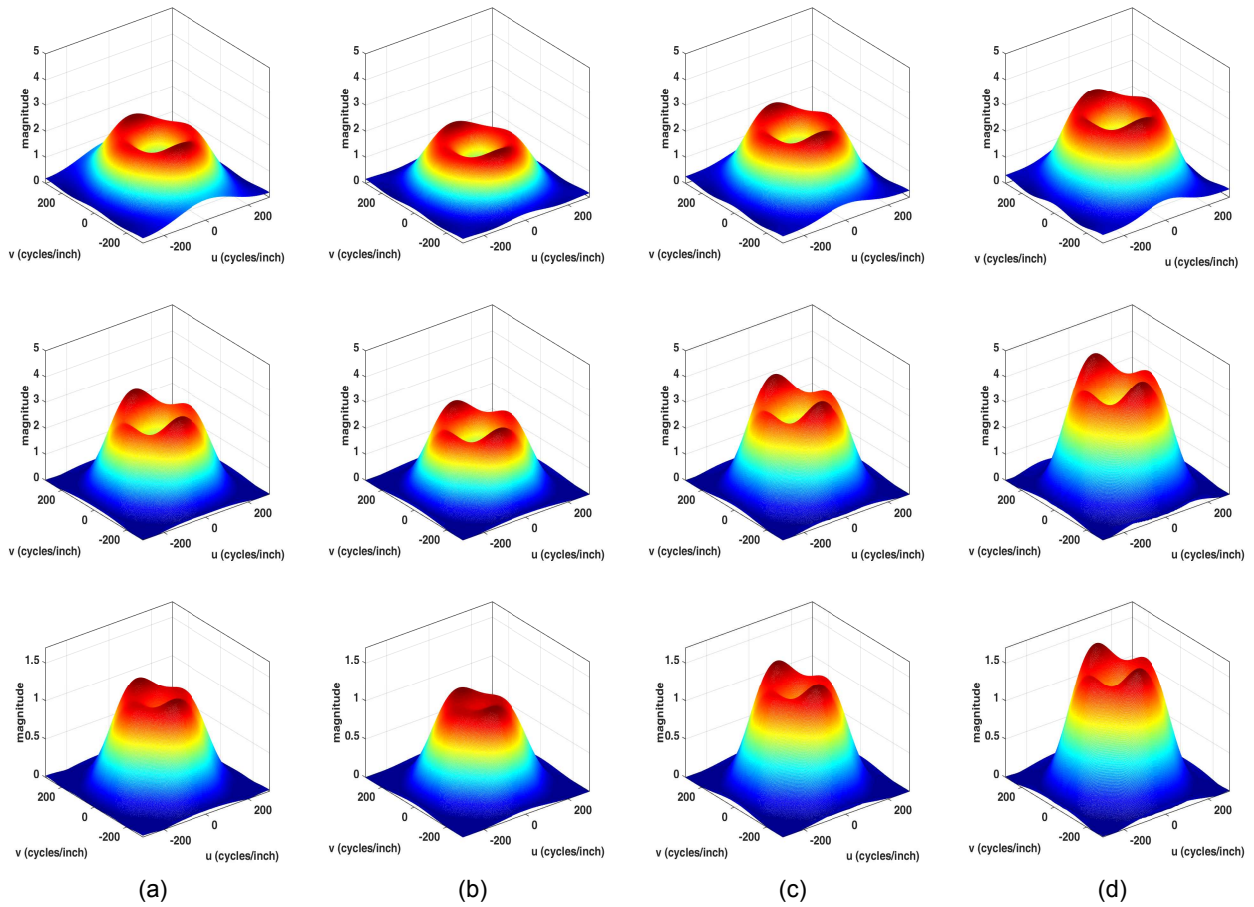


Figure 6. Quality filters for different scanners: (a) scanner A, (b) scanner B, (c) scanner A with Gaussian blur $\sigma = 0.5$ and (d) scanner A with Gaussian blur $\sigma = 0.6$. Quality filters achieve consistent quality levels by cascading the individual scanner equalizing characteristics with (top row) a unity reshaping curve, (middle row) a gain reshaping curve, and (bottom row) an attenuation curve. The reshaping curves are shown in Figure 5.

Table 1. Sharpness levels measured from the original (not equalized) scanners and after applying different gains and attenuations to each of the scanner's equalizing filter responses.

Image	Scan A	Scan B	Smooth A ($\sigma = 0.5$)	Smooth A ($\sigma = 0.6$)
CPBDM (Not Equalized)	0.8120	0.8471	0.5921	0.4519
CPBDM (Equalized)	0.9326	0.9369	0.9227	0.9260
CPBDM (Equalized with Gain)	0.9505	0.9669	0.9463	0.9504
CPBDM (Equalized with Attenuation)	0.8499	0.8376	0.8204	0.8321

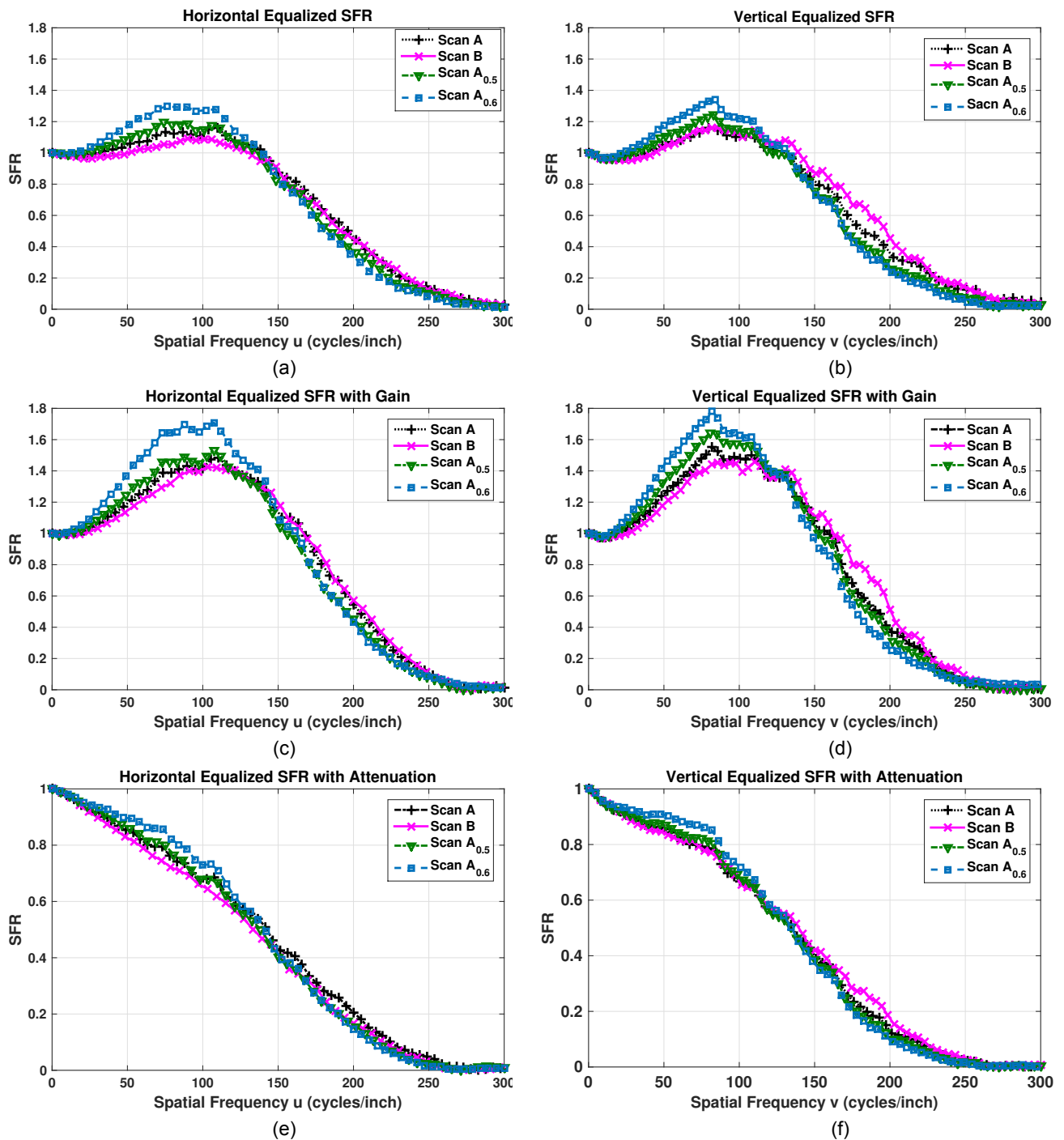


Figure 7. Measured SFRs (each horizontal and vertical) of quality filters of Figure 6, after applying quality filters with (a,b) unity reshaping curve, (c,d) gain reshaping curve, and (e,f) attenuation reshaping curve.

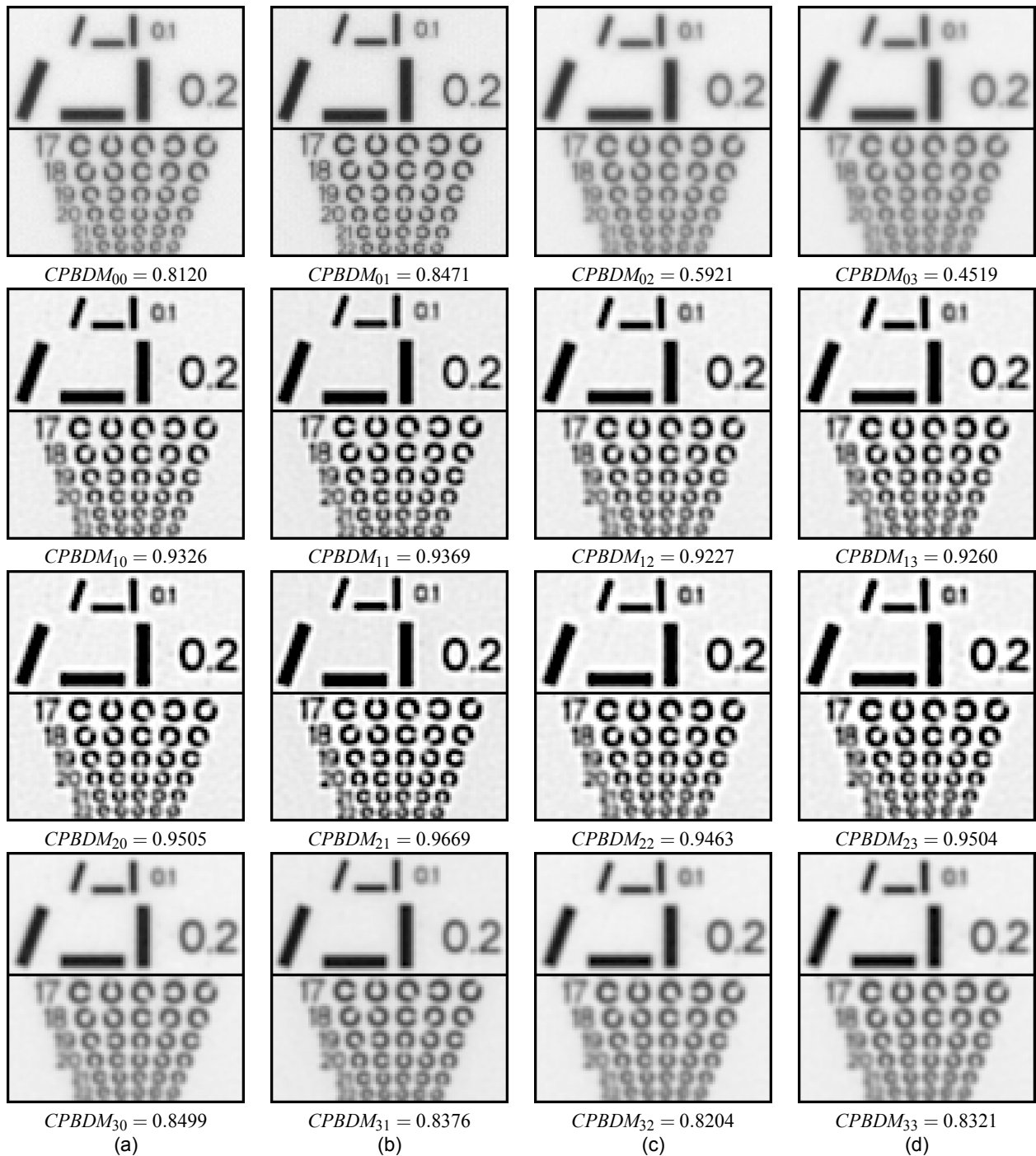


Figure 8. Enhanced images using different quality filters for each test scanner. The sharpness measure CPBDM is shown for each image corresponding to Table 1. Columns (a), (b), (c), and (d) correspond respectively to scanners A, B, A with Gaussian blur $\sigma = 0.5$, and A with Gaussian blur $\sigma = 0.6$. Top, upper middle, lower middle, and bottom rows correspond respectively to non-equalized (original), equalized (i.e., unity reshaping curve), equalized with gain, and equalized with attenuation.